Hindered Diffusion of Flexible Polymers Through Polyimide Ultrafiltration Membranes

M. A. M. BEERLAGE,[1] J. M. M. PEETERS,[2] J. A. M. NOLTEN,[3] M. H. V. MULDER,[3] H. STRATHMANN[3]

[1] KEMA, Utrechtseweg 310, 6812 AR Arnhem, The Netherlands

[2] Sigma Coatings Research Amsterdam, PO Box 58061, 1040 HB Amsterdam, The Netherlands

[3] University of Twente, Faculty of Chemical Technology, P.O. Box 217, 7500 AE, Enschede, The Netherlands

Received 13 March 1998; accepted 9 July 1999

ABSTRACT: The hindered diffusion of polystyrene in dilute solutions of ethyl acetate through polyimide ultrafiltration membranes has been investigated. The present system did not show specific membrane-solute interactions; furthermore, polystyrene can be considered as a flexible polymer coil. It is shown that the hindered diffusive permeability for monodisperse dilute solutions for a series of molecular weights can be compared well with the diffusive permeability curve of one polydisperse dilute polystyrene solution. In the case of very dilute solutions, the polymer coils have no interaction with each other, and the whole range of molecular-weight-dependent permeabilities can be determined from only one measurement. The diffusion behavior of polydisperse solutions through various polyimide membranes has been investigated as well. It was found that the diffusive permeability curve is strongly dependent on the type of membrane, that is, on the pore size distribution. It was not possible to calculate a pore size distribution from diffusion experiments due to mathematical limitations. Nevertheless, it was shown that hindered diffusion measurements are useful to estimate a maximum pore size for each membrane. © 2000 John Wiley & Sons, Inc. J Appl Polym Sci 75: 1180–1193, 2000

Key words: membrane characterization; ultrafiltration; hindered diffusion

INTRODUCTION

Characterization of ultrafiltration membranes is still prone to several experimental and theoretical problems, like membrane-solute or solute-solvent interactions, flow-induced deformation of flexible solutes, the occurrence of concentration polarization, and the necessity for some methods to dry the membranes (e.g., gas permeation and perm-porometry). A comparison of characterization techniques for nonaqueous systems with those for aqueous systems reveals many additional problems. In nonaqueous systems, many disturbing interactions can be prevented by choosing the right model system.

In this article, transport measurements will be described for dilute solutions of polystyrene in ethyl acetate, in the absence of convection. Since the transport mechanism through the membrane is exclusively diffusive, flow-induced deformation of the polystyrene chains (caused by convection[1]) will not occur. The measurements are performed at very low feed concentrations, which means that the chains have no interaction with each other. Diffusion of polystyrene molecules through a porous membrane is strongly hindered; the theory of

Correspondence to: M. H. V. Mulder.

Journal of Applied Polymer Science, Vol. 75, 1180–1193 (2000)
 CCC 0021-8995/00/091180-14

hindered diffusion of flexible polymers through porous systems will be reviewed shortly in the theoretical part of this article.

Polystyrene (PS) has been chosen as a model polymer for three reasons. First, there are many publications in literature on the diffusive behavior of this system, and PS may be considered as a polymer coil without long-range interactions with most membrane materials. Second, PS is commercially available in both monodisperse fractions and with a broad molecular weight distribution. Third, there are many data available on radii of gyration, bulk diffusion coefficients, and solvent quality of polystyrene solutions.

Diffusion of mono- and polydisperse polystyrene solutions in various membranes will be compared. The possibility to use diffusion measurements for the determination of pore size distributions in ultrafiltration membranes will also be discussed.

THEORETICAL BACKGROUND

Hindered Diffusion of Rigid Particles in Porous Systems

Diffusion of particles inside the pores of a porous medium, like a membrane, is highly hindered because of the increased friction by the presence of a confining pore wall. Furthermore, the partition coefficient between bulk and pore is of importance for the overall diffusive transport, too. When particles are large enough, steric exclusion might take place, which turns the diffusivity to zero. With smaller particles, the distribution inside and outside the pores can be influenced by steric effects and long-range intermolecular forces.

The hindrance factor H (with $0 < H < 1$) is defined as D_m/D_o, where D_m is the effective diffusion coefficient through the porous membrane and D_o is the bulk diffusion coefficient. H is often related to λ_s, that is, the ratio of the solute Stokes–Einstein radius to the pore radius is as follows: $\lambda_s = r_s/r_p$. As an example, the Renkin equation is given here[2,3] as follows:

$$\frac{D_m}{D_o} = H = K_R f_R = (1 - \lambda_s)^2(1 - 2.1044\ \lambda_s + 2.0888\ \lambda_s^3 - 0.948\ \lambda_s^5) \quad (1)$$

For a solute that is only 0.1 times the pore size, that is, $\lambda_s = 0.1$, the calculated diffusion hindrance factor is already 0.64, which has been confirmed experimentally by Deen.[4]

In practice, the Renkin equation describes quite accurately the transport of spherical rigid particles (e.g., asphaltenes[5]), crosslinked macromolecules,[6,7] or small macromolecules with $\lambda_s < 0.4$ through cylindrical pores.[6–8]

However, problems arise when charges are involved or other pore shapes are applied. Malone and Anderson[9] described the hindered diffusion of latices through rhombic (diamond-shaped) pores. Their results indicate that the charged latices, influenced by surfactants and solution ionic strength, show a much higher hindrance factor than similar neutral particles. A correction factor was found necessary for the rhombic pore shape. Weinbaum[10] and Pawar and Anderson[11] calculated hindered diffusion in slit-shaped pores.

Robertson and Zydney[12] measured hindered BSA diffusion in asymmetric polymeric membranes; they also found a higher hindrance than was predicted by hard-sphere theories due to charge effects.

In literature, many modifications based on the Renkin equation can be found. Deen[4] wrote an excellent and extensive review on the theory of hindered diffusion and convection of large molecules in porous systems.

Hindered Diffusion of Flexible Macromolecules in Porous Systems

Flexible polymers in solution are regarded as random coils instead of rigid spheres. The size of such a coil is usually indicated as the radius of gyration r_g, which is a statistical average of all kinds of configurations the coil can adopt. Flexible polymers are allowed to diffuse through pores with pore sizes smaller than the radius of gyration. The hydrodynamic radius of a polymer coil r_h is defined as the Stokes–Einstein radius (r_s) of a rigid spherical particles that has the same bulk diffusion coefficient. It is assumed that the diffusion of a polymer through pores that are smaller than its hydrodynamic radius is negligible; that is, the diffusion is effectively zero when $\lambda_s > 1$.

Based on the ideas of Debye and Bueche[13] and Brinkman,[14] Davidson and Deen[15] considered a polymer random coil as a porous body that is permeable for solvent molecules (for this reason, generally, the radius of gyration is somewhat larger than the Stokes–Einstein radius, which is defined for an impermeable rigid sphere). They proposed a model for the hindrance factor for

flexible polymers, based on the variable $\lambda_g = r_g/r_p$, which is the ratio of the radius of gyration of the solute to the pore radius. For flexible polymers, eq. (1) becomes

$$\frac{D_m}{D_o} = H = K_F f_F \tag{2}$$

Here, the index F stands for flexible. Both the partition coefficient of a flexible polymer coil K_F and the wall drag coefficient of a flexible polymer coil f_F are functions of λ_g. The partition coefficient K_F was described analytically by Casassa for cylindrical pores using random-flight statistics,[16] as follows:

$$K_F(\lambda_g) = 4 \sum_{m=1}^{\infty} -\frac{1}{\beta_m^2} \exp\left(-\beta_m^2 \frac{\langle r_g^2 \rangle}{r_p^2}\right) \tag{3}$$

Here, β_m is the mth root of the zeroth-order Bessel function $J_o(\beta) = 0$; $\langle r_g^2 \rangle$ is the mean square of the radius of gyration of the polymer. Results from a Monte Carlo approach[17] were in good agreement with the results of Casassa. The calculated results for the partition coefficient show that when the equivalent $\lambda_s < 0.4$, the value for a porous polymer coil is close to that of a rigid sphere, which explains the rigid sphere-like behavior of macromolecules at low λ_s.

A wall drag coefficient for flexible polymers inside a confining pore has been deduced by Davidson and Deen, based on a porous-body friction coefficient in bulk solution that was derived by Wiegel and Mijnlieff.[18] This modified friction coefficient f_F gives a concentration distribution of the polymer inside the pore. The distribution combined with a set of equations that describe the flow past a stationary solute determines the wall friction.[15] f_F is only dependent on α and λ_g. α is a dimensionless measure of the resistance to solvent flow through the porous-body polymer and is dependent on the polymer–solvent combination and the molecular weight of the polymer. For most polymer–solvent systems, $10 \leq \alpha \leq 60$,[15] where, in general, α is low for a polymer in a good solvent, and α is high for a polymer in poor solvent. In addition, this approach led to a relation between r_s and r_g (and, consequently, between λ_s and λ_g), as follows:

$$\frac{r_s}{r_g} = \frac{2}{3}\sqrt{\frac{2}{3a}}\,\alpha\xi\{\alpha\} \tag{4}$$

Here, $a[-]$ is a measure of the solvent quality.[19]

By using some experimental values for r_s/r_g from the literature, combined with numerical solutions for the $\xi\{\alpha\}$-functions and $f_{F,o}$ for porous spheres in bulk solution, diffusive hindrance factor curves were calculated as a function of λ_s (and λ_g) for three discrete values of α, $\alpha = 10$, $\alpha = 34$, and $\alpha = 60$. These calculations made it clear that H as a function of λ_s of a flexible polymer is smaller than H as a function of λ_s of a rigid solid sphere.

Davidson and Deen also reasoned that for a given polymer, the choice of solvent has only a little effect on the diffusive hindrance, based on entropic and hydrodynamic considerations; as a result, the H-curves for $\alpha = 34$ and $\alpha = 60$ are almost similar.

Diffusion of flexible polymers through pores can also be described by a scaling analysis.[20] For long-chain flexible polymers in good solvents with $r_f \geq r_p$ (with r_f as the Flory radius, i.e., the root mean square end-to-end distance of the chain), the following scaling law was obtained:

$$\frac{D_m}{D_o} = H \cong \alpha'\left(k'\frac{r_f}{r_p}\right)^{-2/3} e\left(-k'\frac{r_f}{r_p}\right)^{5/3} \tag{5}$$

Here, α' and k' are proportionality factors. Equation (5) is a scaling law, which means that it is not possible to predict exact numerical coefficients.[21] Nevertheless, Cannell and Rondelez[22] and Guillot et al.[23] were able to fit their experimental data of diffusion of polystyrene (PS) with $\lambda_s < 1$ in ethyl acetate through Nuclepore membranes using eq. (5).

This scaling approach is especially useful for higher polymer concentrations, when the bulk concentration (c_o) approaches the overlap concentration c^*[21] or even exceeds it. Below c^*, the polymer coils have no interaction with each other and can be treated as independent molecules. The overlap concentration is dependent on the polymer molecular weight.

Scaling arguments predict for semidilute solutions the possibility of large chains to enter pores even if $r_h > r_p$ because the typical hydrodynamic size of a polymer above the overlap concentration is no longer the Stokes–Einstein radius, but a smaller radius that decreases with increasing concentration.[24–26] In this study, attention will be focused only on dilute concentrations, so with $c_o \ll c^*$.

A comparison between the porous-body approach and the scaling analysis is difficult be-

cause they apply to a different regime. The porous-body approach is limited for $\lambda_s \leq 1$, while the scaling analysis was derived especially for cases in which $\lambda_s > 1$.

Experimental Diffusion Studies from Literature

Experimental diffusion data for dilute solutions of polystyrene in ethylacetate through track-etched polycarbonate membranes were obtained by Cannell and Rondelez,[22] Guillot et al.[23] and Guillot.[26] These PS samples were commercially available monodisperse fractions, with molecular weights ranging from $1.07 * 10^5$ to $20.6 * 10^6$ g mol. The λ_s-values, defined as r_h/r_p with r_h as the hydrodynamic radius determined by quasi-elastic light scattering, varied from 0.1 to 0.993.

The scaling approach was used to fit the experimental data.

Kathawalla and Anderson[27] measured diffusion of dilute monodisperse PS solutions in tetrahydrofuran (THF) through track-etched mica membranes with rhombic pores ($\lambda_s < 1$). Their results agree qualitatively well with the results of Cannell and Rondelez and Guillot et al.

In a later article, Kathawalla et al.[28] described the hindered diffusion of disk-like porphyrin molecules in chloroform and of low-molecular-weight polystyrenes ($M_w < 7000$ g mol) in THF ($\lambda_s < 1$). The short-chain polystyrenes were hindered less than the long-chain polystyrenes (M_w: $10^5 - 10^6$ g mol) that were described in the previous article; these short-chain polymers can better be described as rigid rods than as random coils.

Bishop et al.[29] and Teraoka et al.[30] used dynamic light scattering to measure directly the diffusion of polystyrene in a 2-fluorotoluene through porous glasses. Their results are also consistent with the previously mentioned studies.

In addition, Teraoka et al. were able to determine diffusion coefficients of PS inside the pores. They found that when the feed concentration is lower than 20% of the overlap concentration ($c_o < 0.2\ c^*$), the diffusive behavior is almost constant, indicating a dilute concentration regime inside the pores. In practice, this means that feed concentrations should never exceed $0.2\ c^*$ to avoid disturbing semidilute diffusive effects.

Deen et al.[7] and Bohrer et al.[6] measured the hindered diffusion of dextran and ficoll, a crosslinked polysaccharide, in water through polycarbonate track-etched membranes. For dextran, the H-λ_s-curve was significantly higher than the curve for rigid spheres. Deen[4] suggested that interactions between the dextran molecules and the pore wall material cause the increase in the value of H. Davidson et al.[17] theoretically showed by Monte Carlo simulations that even weak interactions drastically increase the partition coefficient. The presence of interactions causes an increase in friction with the pore wall, which should result in a decrease in the value of H. That experimental results show an increase in H means that the influence of interactions on the partition coefficient is larger than that on the wall drag coefficient.

The diffusive hindrance curve for linear polyisoprenes ($\lambda_s < 1$) in amyl acetate, as measured by Bohrer et al.,[31] was situated slightly above the curve for rigid spheres. They also determined hindrance curves for branched, star-shaped polyisoprenes, which were in agreement with the results described previously for polystyrene. In this case, the discrepancy cannot be explained by interactions because linear and star-branched polyisoprenes are supposed to be chemically identical. It is not yet clear where this discrepancy originates from.

Diffusion Experiments Using Asymmetric Membranes

Diffusion experiments are usually carried out in a simple diffusion cell, consisting of two compartments separated by a membrane. One compartment is filled with a dilute polymer solution, while the other contains pure solvent only. These solutions are stirred well to enable a uniform concentration. In the case of polystyrene as diffusing polymer, the stirring rate cannot exceed a certain value because of a possible cleavage of the polymer chain.[32–34]

Because of a concentration gradient, the polymer diffuses through the membrane. From a mass balance, eq. (6) can be derived[35] as follows:

$$\ln \frac{(c_f - c_d)_o}{(c_f - c_d)_t} = \frac{A}{R_{\text{tot}}}\, t\left(\frac{1}{V_f} + \frac{1}{V_d}\right) \tag{6}$$

where c_f and c_d are the polymer concentrations [g/L] on the solution (feed) side and the solvent (diluate) side, respectively. A is the membrane surface area [m^2], and V_f and V_d are the volumes of the two compartments [m^3]. The subscripts o and t indicate the concentration differences at time zero and time t, respectively.

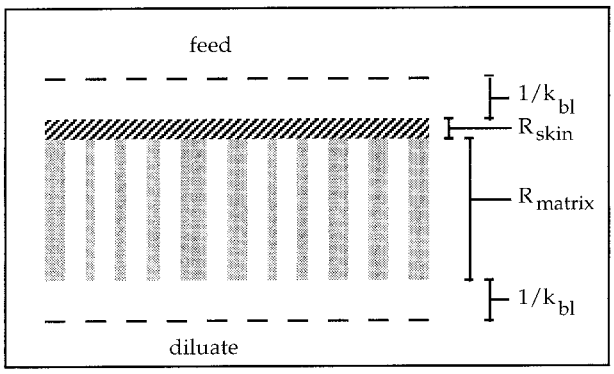

Figure 1 Schematic overview of resistances to diffusive transport through a membrane, plus two boundary layers (at the well-mixed feed and the diluate side).

R_{tot} [s/m] is the total resistance to diffusive transport. The total diffusive permeability, P_{tot} [m/s], is the inverse of the total diffusive resistance. When diffusion results are plotted as the logarithm of the ratio of the concentration differences in the feed and diluate versus the diffusion time t, a straight line is the result with a slope of $(A/R_{tot}) * (1/V_f + 1/V_d)$.

R_{tot} is the summation of the resistances of the membrane and boundary layers, the feed and diluate phase (resistance in series), and can be represented by

$$R_{tot} = \frac{1}{k_{tot}} = \frac{1}{k_{feed}} + \frac{2}{k_{bl}} + \frac{1}{k_{membr}} + \frac{1}{k_{diluate}} \quad (7)$$

Since the feed and diluate phase are well mixed,

$$R_{tot} \approx \frac{2}{k_{bl}} + \frac{1}{k_{membr}} = \frac{2}{k_{bl}} + R_{matrix} + R_{skin} \quad (8)$$

where k_{bl} [m/s] is the mass transfer coefficient of the liquid boundary layers on both sides of the membrane.

The asymmetric membrane consists of a thin symmetric top layer with a diffusive resistance R_{skin} and a thicker symmetric support layer with a diffusive resistance R_{matrix}. The resistances are assumed to be in series, and a schematic drawing of the process is given in Figure 1.

The boundary layer mass transfer coefficient in a stirred cell can be described by[36] the following:

$$k_{bl} b_{cell} = 0.285\ D_o * \left(\frac{\nu}{D_o}\right)^{0.33} * \left(\frac{\omega b_{cell}^2}{\nu}\right)^{0.57} \quad (9)$$

where b_{cell} is the radius of the compartment of the diffusion cell [m], ν is the kinematic viscosity [m^2/s], and ω is the stirring speed [/s]. Equation (9) is only valid for a ratio of cell radius to stirrer bar radius of 1.11,[36] which is equal to the ratio used in the present study.

The resistance of the polymer matrix can be represented by eq. (10), assuming that the matrix consists of symmetric straight cylindrical pores of radius r_{matrix} [m], as follows:

$$R_{matrix} = \frac{l_{matrix}}{n_{matrix} \pi r_{matrix}^2 * D_{matrix\ pore}} \quad (10)$$

where l_{matrix} is the length [m] of the matrix pores ($\approx$ membrane thickness), n_{matrix} is the number of matrix pores per membrane surface area [/m^2], $n_{matrix} \pi r_{matrix}^2$ is equal to the matrix porosity$j$ $\varepsilon_{matrix}[-]$, *and* $D_{matrix\ pore}$ is the effective diffusion coefficient of the solute in the matrix pore [m^2/s].

The resistance of the skin is determined by the following two factors: the diffusion resistance by the top layer, combined with entrance, and exit effects to diffusion into and out of the pores. Entrance and exit effects each add an equivalent length of $0.25 * \pi * r_p$ to the diffusion path.[37] Assuming that the top layer is a symmetric layer with straight cylindrical pores of radius r_p [m] and pore length or skin thickness l_{skin} [m], the resistance of the skin becomes[37]

$$R_{skin} = \frac{l_{skin}}{n_{skin} \pi r_p^2 D_p} + \frac{0.5\ \pi r_p}{n_{skin} \pi r_p^2 D_o} \quad (11)$$

where D_p is the diffusion coefficient inside the skin pores [m^2/s], n_{skin} is the number of pores in the skin per membrane surface area [m^2] and $\Sigma n\{r_p\} \pi r_p^2$ is a measure of the pore size distribution in the top layer.

It will be shown below that the resistances of the boundary layers and of the matrix are negligible compared to the resistance of the skin (see the Experimental Section). The total diffusive permeability for a solute is then given by the inverse of the top layer resistance; the permeability is determined experimentally by monitoring the concentration difference in time, according to eq. (6). The effective diffusion coefficient through the membrane is, in that case, equal to the diffusion coefficient inside the skin pores: $D_m = D_p$.

Measurements are carried out in the dilute regime, which implicitly excludes the possibility of concentration-induced deformation.

The Stokes–Einstein radius, which is the radius of a rigid sphere that is impermeable to solvent molecules, is taken as the hydrodynamic radius of the polymer. This is the smallest size a polymer coil can adopt in a dilute solution. This implies that a polymer chain in a dilute solution cannot diffuse through a membrane pore with a radius smaller than the hydrodynamic radius. The pore size distribution of the accessible pores for a certain polymer is between r_h as a minimum and $r_{p,\max}$ as a maximum. r_h depends on the polymer molecular weight via the hydrodynamic radius, while $r_{p,\max}$ is the largest pore radius that is present in the membrane, which is a fixed value that is determined only by the membrane morphology.

In principle, $r_{p,\max}$ can be determined by diffusion measurements, as follows: it is equal to r_h of the largest polymer molecule that can pass through the membrane, which is the highest molecular weight that can be detected at the diluate side. Based on eq. (11), the permeability of the polymer a, with the maximum molecular weight that is still permeable, can be represented by eq. (12), as follows:

$$P_a = \frac{n_{p,a}\pi r_{p,a}^2 D_p\left\{\frac{r_{h,a}}{r_{p,a}}\right\} D_{o,a}}{l_{\text{skin}} D_{o,a} + 0.5\pi r_{p,a} D_p\left\{\frac{r_{h,a}}{r_{p,a}}\right\}} \tag{12}$$

Here, the braces indicate that D_p is a function of $r_{h,a}/r_{p,a}$. When values are obtained for the skin thickness, l_{skin} (estimated from scanning electron microscopy) and the bulk diffusion coefficient $D_{o,a}$ (from literature), an estimation of D_p as a function of solute size to pore size ratio, $r_{h,a}/r_{p,a}$ (from theory), provides us the number of pores with radius $r_{p,a}$ ($= r_{p,\max}$): $n_{p,a}$.

A slightly smaller polymer chain b can then pass through somewhat smaller pores ($r_{p,b} < r_{p,a}$), but also through the pores that were already accessible for polymer a. The effective diffusion coefficient of b through these largest pores is larger than the diffusion coefficient of a: the solute size to pore size ratio (pore size ($r_{p,a}$) is smaller for polymer b than for polymer a.

Now for polymer b, the permeability is given by

$$P_b = \frac{n_{p,a}\pi r_{p,a}^2 D_p\left\{\frac{r_{h,b}}{r_{p,a}}\right\} D_{o,b}}{l_{\text{skin}} D_{o,b} + 0.5\pi r_{p,a} D_p\left\{\frac{r_{h,b}}{r_{p,a}}\right\}} + \frac{n_{p,b}\pi r_{p,b}^2 D_p\left\{\frac{r_{h,b}}{r_{p,b}}\right\} D_{o,b}}{l_{\text{skin}} D_{o,b} + 0.5\pi r_{p,b} D_p\left\{\frac{r_{h,b}}{r_{p,b}}\right\}} \tag{13}$$

and

$$D_p\left\{\frac{r_{h,b}}{r_{p,a}}\right\} > D_p\left\{\frac{r_{h,b}}{r_{p,b}}\right\}$$

For the smallest polymer n, the permeability is given by

$$P_n = \sum_{i=1}^{n}\left(\frac{n_{p,i}^*\pi r_{p,i}^2 D_p\left\{\frac{r_{h,n}}{r_{p,i}}\right\} D_{o,n}}{l_{\text{skin}} D_{o,n} + 0.5\ \pi r_{p,i} D_p\left\{\frac{r_{h,n}}{r_{p,i}}\right\}}\right) \tag{14}$$

The values of the number of pores $n_{p,i}^*$ are indicated with an asterisk, and they have to be calculated for each step in pore size.

The summation of $n_{p,i}^*\pi r_{p,i}^2$ over all pore sizes gives the pore size distribution of the membrane; eq. (14) shows the dependence of the diffusive permeability on the membrane pore size distribution. In fact, it should be possible to estimate a pore size distribution from a diffusive permeability measurement of a polymer with a broad molecular weight distribution. However, the intricate dependence of the effective diffusion coefficient on the solute size to pore size ratio will be a complicated factor, and is not well defined.

A certain period of time will be required to allow the higher-molecular-weight polymer chains to diffuse.

Furthermore, the effect of a polydisperse feed solution has to be investigated (most literature data were obtained with monodisperse polymer fractions). Guillot,[38] until now, was the only one who reported both on monodisperse solutions and solutions of mixtures of two molecular weights. He found that in the dilute regime, a solute molecule with a certain M_w did not influence the diffusion kinetics of a molecule with a different molecular weight. An increase of the concentration of one of the components close to the overlap concentration c^* resulted in a blockage of small

solutes by large solutes or a diffusion enhancement of large solutes by small solutes.

EXPERIMENTAL

Membranes and Materials

PI-powder (P84, Lenzing AG, Austria, 325-mesh, chargenr. 8170914) was dried at least 24 h at 150°C in vacuum before preparation of the casting solutions. Solutions of 20 wt % of PI with 3 wt % of tartaric acid in dimethylformamide (DMF) were prepared immediately after the drying procedure, and the air inside the conical flask was replaced by nitrogen. After 24 h of stirring (without heating), the solutions were filtered with a Bekipor® 25-μm stainless steel filter from Bekaert Corp. The solutions were degassed overnight.

A film of 0.20 mm thickness was cast on a dry and clean glass plate and immediately immersed in the coagulation bath, containing ethanol or demineralized water. The residence time in the bath was at least 10 min, but the membranes precipitated immediately. The prepared membranes were flushed for 24 h with water to remove DMF; the water was replaced by ethanol, in which the membranes were stored.

Before the membranes were applied for filtration of ethyl acetate or polymer solutions in ethyl acetate, they were preconditioned in this liquid for at least 2 days.

Polystyrene Solutions: Characteristics and Concentration Analysis

Six monodisperse polystyrene (PS) samples with molecular weights from 4070 to 1,447,000 g mol were obtained from Aldrich.

The bulk diffusion coefficients [m^2/s] for these samples were obtained by quasi-elastic light scattering[22,39] and fitted using a power law dependence, according to the method that Kathawalla and Anderson[27] used for PS in tetrahydrofuran (THF). An additional temperature and viscosity correction was necessary because the measurements were performed at 25.0°C in our case. Since low-molecular-weight polystyrenes ($M_w < 10{,}000$) can be better considered as rigid rods than as random coils,[28] two power law relations were used; for $M_w > 10{,}000$,

$$D_o \sim 3.296 * 10^{-8} * M_w^{-0.533} \tag{15}$$

for $M_w < 10{,}000$,

$$D_o \sim 1.75 * 10^{-8} * M_w^{-0.511} \tag{16}$$

Hydrodynamic radii (i.e., Stokes–Einstein radii) were calculated from these bulk diffusion coefficients according to the Stokes–Einstein equation. Overlap concentrations are calculated according to two methods: eq. (17) represents the c^*, as given by Doi and Edwards[40] (c^{*a}), while eq. (18) is the estimation des Cloizeaux and Jannink used[41] (c^{*b}), as follows:

$$c^{*a} = \frac{M_w}{\frac{4}{3}\pi r_g^3 N_A} \tag{17}$$

$$c^{*b} = \frac{M_w}{(\sqrt{2}\, r_g)^3\, N_A} \tag{18}$$

Here, N_A is Avogadro's number, and r_g is the radius of gyration; r_g was estimated from relation (19), which is applicable for good solvents,[42–44] as follows:

$$\frac{r_g}{r_h} = 1.48 \pm 0.03 \tag{19}$$

The characteristics of the various monodisperse polystyrenes and the feed concentrations are summarized in Table I. The values of M_w/M_n are a measure of the polydispersity, that is, the ratio of the weight-average molecular weight to the number-average molecular weight.

Below the overlap concentration c^*, polymer chains have no interaction with each other. The concentrations of the feed solutions were in all cases far below the overlap concentration ($c_o < 0.2\ c^*$). The concentrations of solutions at the diluate side were determined by ultraviolet (UV) spectrophotometry (Philips PU UV/Vis 8720 Scanning Photospectrometer) at a wavelength of 260 nm. Samples were returned to the diffusion cell after analysis.

A commercially available polystyrene was purchased from BDH-Chemicals with a broad molecular weight distribution for diffusion measurements of polydisperse PS-solutions (see Fig. 2).

The feed concentrations during these measurements was about 2 g/L. Samples at the diluate side were analyzed with gel permeation chromatography (GPC), consisting of a high pressure

Table I Characteristics of the Various Monodisperse Polystyrenes Used

M_w (g/mol)	M_w/M_n (−)	D_o (m^2/s)	r_h (nm)	c^{*a} (g/L)	c^{*b} (g/L)	c_o (g/L)
4075	1.04	$2.5 * 10^{-10}$	2.1	57	84	1.76
45,730	1.05	$1.1 * 10^{-10}$	4.8	52	77	3.17
95,800	1.04	$7.3 * 10^{-11}$	7.1	33	50	3.31
401,340	1.02	$3.4 * 10^{-11}$	15.1	14	21	1.72
850,000	1.06	$2.3 * 10^{-11}$	22.5	9.1	14	1.01
1,447,000	1.14	$1.7 * 10^{-11}$	29.9	6.6	9.8	1.00

liquid chromatography (HPLC)-pump (Waters 510) with an autosampler (Hewlett Packard HP 1050 TI), a variable UV detector (Waters 486), a differential refractometer (Waters 411), and two μStyragel-HT columns (Waters 10^4 and 10^5 Å). The total volume of the samples taken from the diluate side was about 3% of the total compartment volume. The diluate compartment was refilled with clean ethyl acetate. The concentrations of the various fractions in the polydisperse sample are much lower than with monodisperse samples, because the overall concentrations are of the same order of magnitude. As a consequence, a small increase in concentration at the diluate side affects the diffusive permeability of other fractions perceptively when polydisperse samples are used. For this reason, only measurements of separate fractions are discussed in which the concentration at the diluate side (c_{dt}) does not exceed 10% of the original feed concentration (c_{fo}).

Samples are taken at different times, varying from 4 to 14 days. The permeability is constant in time, according to eq. (6). To verify this, an example is given in Figure 3, in which the diffusive permeability of a certain PI membrane for polystyrene has been determined after 7 and 14 days, respectively. The small differences in permeability may be ascribed to detection errors.

Diffusion Measurements

The diffusion test cell set-up is schematically drawn in Figure 4. It consists of two glass compartments, which were kept at 25.0°C.

The volume of each compartment was $56 * 10^{-6}$ m^3, and the membrane surface area $13.2 * 10^{-4}$ m^2. The membrane was clamped tightly into the cell using Kalrez® O-rings, to ensure chemical resistance to ethyl acetate and to prevent evaporation. One compartment was filled with the PS-solution, while the other was filled with ethyl acetate. The top layer of the membrane was faced towards the solution side. Refilling and sampling

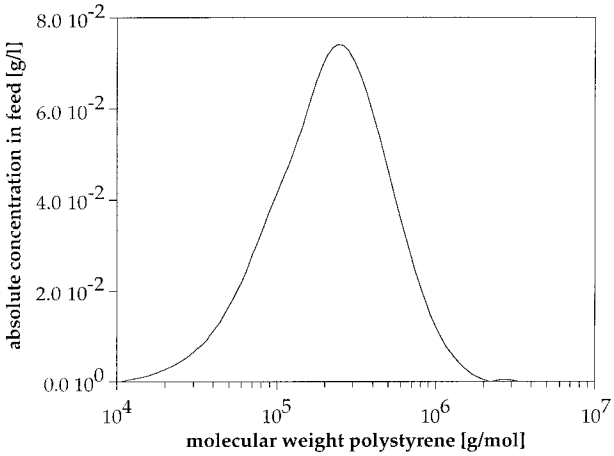

Figure 2 Molecular weight distribution of polydisperse PS as a function of the molecular weight determined by GPC.

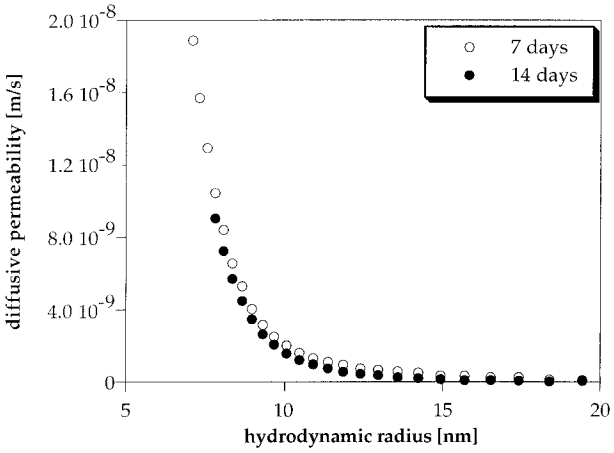

Figure 3 Diffusive permeability of polystyrene in a membrane (made from a casting solution of 20% polyimide in DMF and coagulated in ethanol) after 7 days (open circles) and 14 days (closed circles).

in both compartments was done through Teflon taps. Each compartment contained a magnetic stirrer, which was driven externally. The stirrer speed was set at 180 rpm, and the ratio of the cell radius to the stirrer radius was 1.11.

Sometimes a leak in the membrane was observed, caused by the tight clamping of the membrane. In these cases, the diffusive permeability graphs expressed clearly an independence of P on the molecular weight.

The boundary layer mass transfer coefficient of the high-molecular-weight monodisperse polystyrene was estimated by eq. (9), resulting in $k_{bl} = 2.96 * 10^{-6}$ m/s. The combined resistances of the boundary layers are then $2/k_{bl} = 6.7 * 10^5$ s/m, which is less than 0.1% of the total resistance over the membrane (see below).

To determine the resistance of the membrane matrix , estimations of the thickness and porosity should be made. From a typical scanning electron micrograph (SEM), the following values were obtained: $l_{\text{matrix}} = 75\ \mu$m, $\varepsilon_{\text{matrix}} = 0.80$, and $r_{\text{matrix}} = 200$ nm. Consequently, for a PS chain with $r_h = 15$ nm ($M_w = 401{,}340$), $\lambda_s = 15/200 = 0.08$. Then, from Figure 1, H is determined to be 0.8, so the effective diffusion coefficient of this polymer in the matrix is $0.8 * D_o$, with $D_o = 3.4 * 10^{-11}$ m^2/s.

The resistance of the matrix, R_{matrix}, can now be calculated from eq. (10): $R_{\text{matrix}} = 3 * 10^6$ s/m. A typical value of the total resistance of the membrane for this polymer is, in all experimental cases, more than $1 * 10^9$ s/m, which is more than 300 times higher. For smaller PS molecules, the resistance by the matrix is even less. From these considerations, it may be concluded that the total resistance of the membrane to diffusive transport is almost completely determined by the top layer. Therefore, eq. (11) is valid for this system. One has to keep in mind that a model description is used, where the pores are regarded as straight cylindrical channels. This assumption also applies for other characterization methods like retention measurements or permporometry. In practice, the configurations of the pores are quite different. In addition, there will be a gradient in pore size across the top layer. Introduction of this gradient into eq. (11) means that l_{skin} will be dependent on the pore size as well.

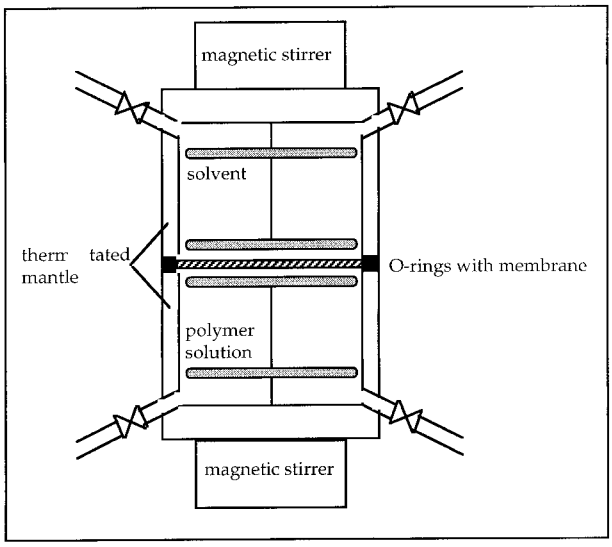

Figure 4 Diffusion measurement set-up.

Table II Diffusive Permeability of Monodisperse Polystyrenes

M_w (g/mol)	r_h (nm)	P (m/s)
4075	2.1	$4.7 * 10^{-8}$
45,730	4.8	$1.4 * 10^{-8}$
95,800	7.1	$6.2 * 10^{-9}$
401,340	15.1	$1.9 * 10^{-9}$
850,000	22.5	$8.9 * 10^{-10}$
1,447,000	29.9	$5.3 * 10^{-10}$

RESULTS AND DISCUSSION

Diffusive Permeability of Monodisperse and Polydisperse Solutions

A batch of similar membranes was used to compare the diffusion of polystyrenes in monodisperse solutions and in polydisperse solutions. For this purpose, films cast from a 20 wt % polyimide solution in DMF containing 3 wt % tartaric acid were coagulated in ethanol. After preconditioning in ethyl acetate, the membranes were installed in the diffusion test cell set-up. For each measurement, a fresh membrane was applied.

If the natural logarithm of the ratio of the concentration differences is plotted versus time for the monodisperse polystyrenes, according to eq. (6), the diffusive permeabilities can be calculated from the slope of each line. The results are summarized in Table II, as a function of the molecular weight M_w and the hydrodynamic radius r_h.

Diffusion measurements with a polydisperse PS-solution were done using membranes from the same batch. Samples were taken from the diluate

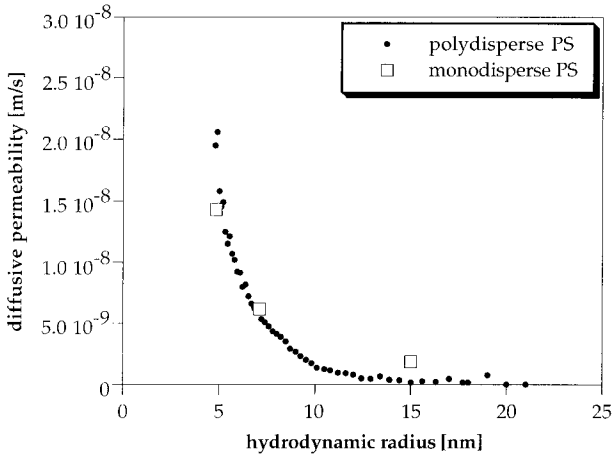

Figure 5 Diffusive permeability of polydisperse polystyrene as a function of the hydrodynamic radius; the monodisperse values are given as reference.

side and analyzed by GPC. The diffusive permeabilities for the different fractions of the polydisperse samples can be calculated in a similar way, using a graphical evaluation of the total resistance to diffusive transport. Figure 5 shows the diffusive permeability as a function of the polymer hydrodynamic radius.

In this graph also, some monodisperse permeabilities are given as comparison, that is, the molecular weights of 45,730, 95,800, and 401,340 g mol.

The concentrations of the highest molecular weight fractions are very low (see Fig. 2), and the determination of the permeability may become inaccurate. It is preferred to employ a more uniform molecular weight distribution as a feed rather than a Gaussian distribution. The concentration of the lowest molecular weights is also very low, but these fractions are already divided over the two compartments after a short period of time, so that the concentration at the diluate side is larger than 10% of the original feed concentration. For this reason, these fractions are not recorded in the diffusive permeability graphs.

From Figure 5, it can be seen that the monodisperse PS permeabilities fit nicely into the polydisperse PS permeabilities. This means that the different fractions in the polydisperse sample do not influence the diffusive permeability of other fractions by blockage or enhanced diffusion; that is, each molecule diffuses independently from the other for solutions in the dilute concentration regime.

The results presented here are in agreement with Guillot's work.[38] Diffusion measurements of a series of monodisperse polymer samples can be approximated by employing a polydisperse polymer, as long as all the separate fractions are below the overlap concentration.

Diffusive Permeability: Suitability as Characterization Technique for Membranes with a Pore Size Distribution

Equation (11) already described the dependence of the diffusive permeability on the membrane pore size distribution for each molecular weight of the polymer. The main conclusion of the last section indicates that the diffusive permeabilities of a polymer with a distribution of molecular weights can be determined by only one experiment. This makes diffusive permeability measurements suitable as characterization technique for ultrafiltration membranes.

In case of a molecular weight distribution, eq. (14) is a summation of n different equations, with n as the number of polymer molecular weight fractions. The objective of this characterization technique is to obtain a permeability for polystyrene as a function of the membrane pore radius r_p, which then can be related to the polystyrene hydrodynamic radius r_h. Therefore, the total diffusive permeability integral, eq. (14), has to be differentiated to r_h. For this purpose, Leibniz's theorem for differentiation of an integral can be used (see the Appendix).

It was already discussed in this article that there are two different theories that describe hindered diffusion. D_p may be determined from the porous body approach, or from the scaling analysis. These theories have in common that D_p is a function of the ratio of the polymer hydrodynamic radius to the membrane pore radius, which means that the diffusive permeability integral function becomes even more complicated.

The diffusive permeability integral cannot be solved analytically, and, also, a numerical solution was not found. However, if one succeeds in finding a solution for this ill-posed mathematical problem (e.g., by making an assumption about the shape of the pore size distribution,[45,46] the diffusive permeability measurements may form a promising ultrafiltration membrane characterization technique, especially for nonaqueous systems where long-range interactions are absent and polymers behave like random coils, so many disturbing effects do not occur. Until then, these measurements are useful to determine a maxi-

mum pore radius for a certain membrane and to compare different membranes qualitatively.

Results of Measurement of Diffusive Permeability for Different Membranes

To verify the dependence of the diffusive permeability on the pore size distribution, various membranes were employed for diffusion experiments of polydisperse PS solutions. In Figure 6, the diffusive permeability curve of a membrane prepared from a 20 wt % polyimide casting solution in DMF and coagulated in ethanol is compared with the curve of a membrane from a 25 wt % polyimide casting solution in DMF that was prepared under equal conditions.

From this figure, it can be seen that the membrane prepared from a casting solution containing 20 wt % PI has a higher diffusive permeability over almost the whole range. The membrane that was prepared from a 25 wt % PI casting solution shows permeability through pores with a radius of about 16 nm. This is probably caused by the presence of pinholes because it is not expected that there are pores present of 16-nm radius. Therefore, the maximum pore radius for this membrane is estimated to be 6 nm. For the membrane cast from a 20 wt % PI solution, a maximum pore radius of about 14 nm was determined.

The pure ethanol hydraulic permeabilities of these membranes, which were determined in a pressure set-up with a *trans*membrane pressure of 1 bar, were 291 kg m^{-2} h^{-1} bar for the membranes cast from a 20 wt % PI-solution and 49 kg m^{-2} h^{-1} bar for membranes cast from a 25 wt % PI-solution, respectively.[47] These convective permeabilities can be related to the diffusive permeability results presented in Figure 6, as follows: the higher permeability of the membrane from a 20 wt % casting solution is caused by the presence of larger pores compared to the membrane from a 25 wt % casting solution.

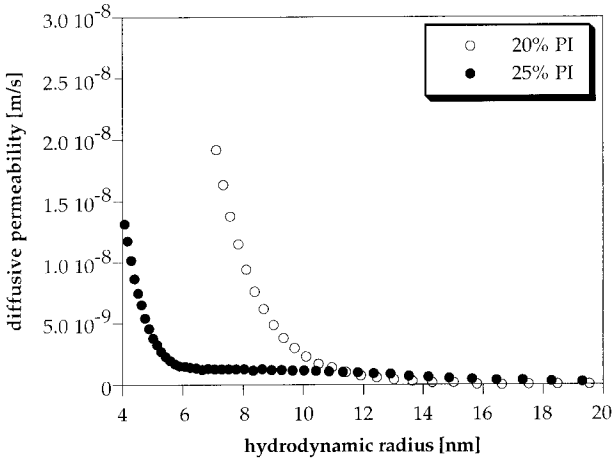

Figure 6 Diffusive permeability for polyimide membranes, prepared from an initial polyimide concentration in the DMF casting solution of 20 and 25 wt %, respectively.

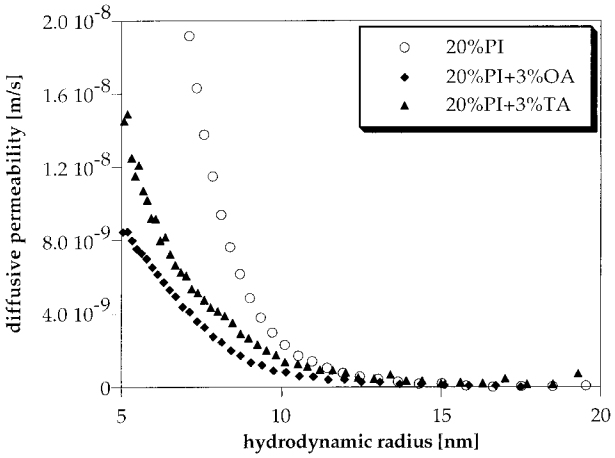

Figure 7 Diffusive permeability of membranes prepared from casting solutions containing 20 wt % polyimide, with and without addition of 3 wt % oxalic (OA) or tartaric acid (TA) to the casting solution.

Previously, it was concluded from polystyrene retention measurements[1] that the major part of the pores of these wet membranes are smaller than 7 nm, and this is quite reasonable when considering that the largest pores are 6 and 14 nm, respectively. Permporometry results for these membranes (after a drying procedure) showed that the maximum pore sizes are about 7 and 14 nm for the membranes prepared from a 25 wt % PI casting solution and prepared from a 20 wt % solution, respectively.[47] This is in agreement with the diffusive permeability results described in this article, which implies that during the drying of these membranes, the radii of the largest pores will hardly change, and that swelling of the membrane by the wetting liquid has only a minor influence.

The diffusive behavior of membranes prepared from 20 wt % polyimide casting solutions is compared with similar membranes that were prepared from 20 wt % polyimide casting solutions containing 3 wt % oxalic acid (OA) or tartaric acid (TA), and the results are given in Figure 7. All membranes were coagulated in ethanol.

From Figure 7, it can be seen that the additives do not influence the maximum pore radius. The lower permeability at lower PS hydrodynamic radius for the additive membranes indicates that the number of pores in this region is drastically decreased by the addition of OA or TA to the casting solution. The effect of OA is stronger than the effect of TA. These findings are in agreement with the results described by Wienk et al.[48] The addition of OA or TA to a 20% polyimide casting solution results in a decline in pure ethanol permeability when compared to membranes casted from solutions without additives. The ethanol permeability decline is stronger for OA than for TA. Furthermore, permporometry results showed that the presence of the additives in the casting solution has only a minor effect on the pore peak maximum, whereas it decreases the number of pores.[47]

CONCLUSION

The diffusive permeabilities of dilute solutions of monodisperse polystyrene fractions in ethyl acetate, measured for polyimide ultrafiltration membranes, correspond well with the diffusion results for a polydisperse polymer for the same membrane.

The experiments were employed to compare qualitatively the hindered diffusion of polystyrene molecules through polyimide membranes. The effect of drying and rewetting of the membranes was studied as well. It was shown that the maximum pore radius that was determined by the diffusive permeability measurements could be related to membrane formation and pretreatment processes. In addition, the results are in qualitative agreement with results obtained by retention and pure ethanol permeability measurements and permporometry.

An attempt was made to calculate membrane pore size distributions from the experimental diffusive permeability curves. Because this is an ill-posed mathematical problem and the description of the diffusion coefficient inside the membrane is not uniform, this was not yet possible. Until these problems are solved, the experimental results can be used to compare maximum pore radii and permeability curves for different membranes.

REFERENCES

1. Beerlage, M. A. M.; Heijnen, M. L.; Mulder, M. H. V.; Smolders, C. A.; Strathmann, H. J Membr Sci 1996, 113, 259.
2. Renkin, E. M. J Gen Physiol 1954, 38, 225.
3. Pappenheimer, J. R.; Renkin, E. M.; Borrero, L. M. Am J Physiol 1951, 167, 13.
4. Deen, W. M. AIChE J 1987, 33, 1409.
5. Baltus, R. E.; Anderson, J. L. Chem Eng Sci 1983, 38, 1959.
6. Bohrer, M. P.; Patterson, G. D.; Carroll, P. J. Macromolecules 1984, 17, 1170.
7. Deen, W. M.; Bohrer, M. P.; Epstein, N. B. AIChE J 1981, 27, 952.
8. Beck, R. E.; Schultz, J. S. Biochim Biophys Acta 1972, 255, 273.
9. Malone, D. M.; Anderson, J. L. Chem Eng Sci 1978, 33, 1429.
10. Weinbaum, S. Lect Math Life Sci 1981, 14, 119.
11. Pawar, Y.; Anderson, J. L. Ind Eng Chem Res 1993, 32, 743.
12. Robertson, B. C.; Zydney, A. L. J Membrane Sci 1990, 49, 287.
13. Debye, P.; Bueche, A. M. J Chem Phys 1948, 16, 573.
14. Brinkman, H. C. Appl Sci Res 1947, A1, 27.
15. Davidson, M. G.; Deen, W. M. J Membr Sci 1988, 35, 167.
16. Casassa, E. F. J Polym Sci 1967, B5, 773.
17. Davidson, M. G.; Suter, U. W. Macromolecules 1987, 20, 1141.
18. Wiegel, F. W.; Mijnlieff, P. F. Physica 1977, 89A, 385.
19. Mijnlieff, P. F.; Wiegel, F. W. J Polym Sci, Polym Phys Ed 1978, 16, 245.
20. Daoud, M.; de Gennes, P. G. J Phys (Paris) 1977, 38, 85.
21. de Gennes, P. G. Scaling Concepts in Polymer Physics; Cornell University Press: Ithaca, NY, 1979.
22. Cannell, D. S.; Rondelez, F. Macromolecules 1980, 13, 1599.
23. Guillot, G.; Leger, L.; Rondelez, F. Macromolecules 1985, 18, 2531.
24. de Gennes, P. G. Macromolecules 1976, 9, 587.
25. Daoud, M.; Cotton, J. P.; Farnoux, G.; Jannink, G.; Sarma, G.; Benoit, H.; Duplessix, R.; Picot, C.; de Gennes, P. G. Macromolecules 1975, 8, 804.
26. Guillot, G. Macromolecules 1987, 20, 2600.
27. Kathawalla, I. A.; Anderson, J. L. Ind Eng Chem Res 1988, 27, 866.
28. Kathawalla, I. A.; Anderson, J. L.; Lindsey, J. S. Macromolecules 1989, 22, 1215.
29. Bishop, M. T.; Langley, K. H.; Karasz, F. E. Macromolecules 1989, 22, 1220.
30. Teraoka, I.; Langley, K. H.; Karasz, F. E. Macromolecules 1993, 26, 287.

31. Bohrer, M. P.; Fetters, L. J.; Grizzuti, N.; Pearson, D. S.; Tirrell, M. V. Macromolecules 1987, 20, 1827.
32. Müller, A. J.; Odell, J. A.; Carrington, S. Polymer 1992, 33, 2598.
33. Nguyen, T. Q.; Kausch, H. H. Polymer 1992, 33, 2611.
34. Keller, A.; Odell, J. A. Colloid Polym Sci 1985, 263, 181.
35. Cussler, E. L. Diffusion, Mass Transfer in Fluid Systems; Cambridge University Press: New York, 1992.
36. Smith, K. A.; Colton, C. K.; Merril, E. W.; Evans, L. B. Chem Eng Progr Symp Ser 1968, 84, 64, 45.
37. Malone, D. M.; Anderson, J. L. AIChE J 1977, 23, 177.
38. Guillot, G. Macromolecules 1987, 20, 2606.
39. Brandrup, J.; Immergut, E. H. Polymer Handbook, 3rd ed.; Wiley: New York, 1989.
40. Doi, M.; Edwards, S. F. The Theory of Polymer Dynamics; Clarendon Press: Oxford, UK, 1986.
41. des Cloizeaux, J.; Jannink, G. Polymers in Solution: Their Modeling and Structure; Clarendon Press: Oxford, UK, 1990.
42. Fukuda, M.; Fukutomi, M.; Kato, Y.; Hashimoto, T. J Polym Sci, Polym Phys Ed 1974, 12, 871.
43. Nemoto, N.; Makita, V.; Tsunashima, Y.; Kurata, M. Macromolecules 1984, 17, 425.
44. Varma, B. K.; Fujita, Y.; Takahashi, M.; Nose, T. J Polym Sci, Polym Phys Ed 1984, 22, 1781.
45. Mason, E. A.; Wendt, R. P.; Bressler, E. H. J Membr Sci 1980, 6, 283.
46. Leypoldt, J. K. J Membr Sci 1987, 31, 289.
47. Beerlage, M. A. M. Ph.D. Thesis, University of Twente, Enschede, The Netherlands, 1994.
48. Wienk, I. M.; Boom, R. M.; Beerlage, M. A. M.; Bulte, A. M. W.; Smolders, C. A.; Strathmann, H. J Membr Sci 1996, 113, 361.

APPENDIX: DERIVATION OF THE DIFFUSIVE PERMEABILITY INTEGRAL

In this article, polystyrene diffusion experiments through different polyimide membranes were described. The diffusive permeability was shown to be dependent on the membrane pore size distribution. Therefore, these diffusion experiments might, in principle, serve as a technique to characterize ultrafiltration membranes. For this purpose, a relation has to be found between the polymer hydrodynamic radius distribution and the membrane pore size distribution, including the theory of hindered diffusion of flexible polymer chains.

The derivation of this relation, which is presented in this appendix, is based on eqs. (12)–(14); eq. (14) is the basis of a set of n relations describing the diffusive permeabilities of n different polymer hydrodynamic radii through the accessible pores of the membrane. The derivation presented here processes these n relations into one single integral.

For one type of polystyrene molecules i, the diffusive permeability through the pores that are accessible for these molecules, that is, in the interval r_h to infinity, can be written in the form of an integral, as follows:

$$P_{\text{tot},i}\{r_h\} = \int_{r_h}^{\infty} \frac{\frac{dn}{dr}\{r_p\}\pi r_p^2 * D_p\left\{\frac{r_h}{r_p}\right\} * D_o\{r_h\}}{l_{\text{skin}} D_o\{r_h\} + 0.5\ \pi r_p * D_p\left\{\frac{r_h}{r_p}\right\}}\, dr_p \tag{A.1}$$

This is a more generalized form of eq. (14), valid for any molecule i. The bulk diffusion coefficient D_o is written here as a function of the polymer hydrodynamic radius. Note that the number of pores is written here in the differential form, representing the pore size distribution.

To obtain the dependence of the diffusive permeability on the molecular weight, or better the hydrodynamic radius r_h, the integral in eq. (A.1) is differentiated with respect to r_h. For this purpose, Leibniz's theorem for differentiation of an integral is used[A1]:

$$\begin{aligned}\frac{dP_{\text{tot}}}{dr_h}\{r_h\} &= \int_{r_h}^{\infty} \frac{d}{dr_h}\left[\frac{\frac{dn}{dr}\{r_p\}\pi r_p^2 * D_p\left\{\frac{r_h}{r_p}\right\} * D_o\{r_h\}}{l_{\text{skin}} D_o\{r_h\} + 0.5\ \pi r_p * D_p\left\{\frac{r_h}{r_p}\right\}}\right] dr_p \\ &\quad - \left[\frac{\frac{dn}{dr}\{r_h\}\pi r_h^2 * D_p\{1\} * D_o\{r_h\}}{l_{\text{skin}} D_o\{r_h\} + 0.5\ \pi r_h * D_p\{1\}}\right]\end{aligned} \tag{A.2}$$

Further development of the integral results in

$$\begin{aligned}\frac{dP_{\text{tot}}}{dr_h}\{r_h\} &= \int_{r_h}^{\infty} \frac{\frac{dn}{dr}\{r_p\}\pi r_p * \frac{dD_p}{d\left\{\frac{r_h}{r_p}\right\}}\left\{\frac{r_h}{r_p}\right\} * D_o\{r_h\}}{l_{\text{skin}} D_o\{r_h\} + 0.5\ \pi r_p * D_p\left\{\frac{r_h}{r_p}\right\}}\, dr_p \\ &\quad + \int_{r_h}^{\infty} \frac{\frac{dn}{dr}\{r_p\}\pi r_p^2 * D_p\left\{\frac{r_h}{r_p}\right\} * \frac{dD_o\{r_h\}}{dr_h}}{l_{\text{skin}} D_o\{r_h\} + 0.5\ \pi r_p * D_p\left\{\frac{r_h}{r_p}\right\}}\, dr_p\end{aligned}$$

$$- \int_{r_h}^{\infty} \left[\frac{\frac{dn}{dr}\{r_p\}\pi r_p^2 * D_p\left\{\frac{r_h}{r_p}\right\} * D_o\{r_h\}}{\left[l_{\text{skin}} D_o\{r_h\} + 0.5\ \pi r_p * D_p\left\{\frac{r_h}{r_p}\right\} \right]^2} * l_{\text{skin}} * \frac{dD_o\{r_h\}}{dr_h} \right] dr_p$$

$$- \int_{r_h}^{\infty} \left[\frac{\frac{dn}{dr}\{r_p\}\pi r_p^2 * D_p\left\{\frac{r_h}{r_p}\right\} * D_o\{r_h\}}{\left[l_{\text{skin}} D_o\{r_h\} + 0.5\ \pi r_p * D_p\left\{\frac{r_h}{r_p}\right\} \right]^2} * 0.5\ \pi * \frac{dD_p\left\{\frac{r_h}{r_p}\right\}}{d\left\{\frac{r_h}{r_p}\right\}} \right] dr_p$$

$$- \left[\frac{\frac{dn}{dr}\{r_h\}\pi r_h^2 * D_p\{1\} * D_o\{r_h\}}{l_{\text{skin}} D_o\{r_h\} + 0.5\ \pi r_h D_p\{1\}} \right] \tag{A.3}$$

The combination of these five parts finally gives eq. (A.4), as follows:

$$\frac{dP_{\text{tot}}}{dr_h}\{r_h\} = \int_{r_h}^{\infty} \frac{\frac{dn}{dr}\{r_p\}\pi r_p * \left[\frac{dD_p}{d\left\{\frac{r_h}{r_p}\right\}}\left\{\frac{r_h}{r_p}\right\} * D_o\{r_h\} + r_p * D_p\left\{\frac{r_h}{r_p}\right\} * \frac{dD_o\{r_h\}}{dr_h} \right]}{l_{\text{skin}} D_o\{r_h\} + 0.5\ \pi r_p * D_p\left\{\frac{r_h}{r_p}\right\}} dr_p$$

$$- \int_{r_h}^{\infty} \frac{\frac{dn}{dr}\{r_p\}\pi r_p^2 * D_p\left\{\frac{r_h}{r_p}\right\} * D_o\{r_h\} \left[l_{\text{skin}} * \frac{dD_o\{r_h\}}{dr_h} + 0.5\ \pi \frac{dD_p}{d\left\{\frac{r_h}{r_p}\right\}}\left\{\frac{r_h}{r_p}\right\} \right]}{\left[l_{\text{skin}} D_o\{r_h\} + 0.5\ \pi r_p * D_p\left\{\frac{r_h}{r_p}\right\} \right]^2} dr_p$$

$$- \left[\frac{\frac{dn}{dr}\{r_h\}\pi r_h^2 * D_p\{1\} * D_o\{r_h\}}{l_{\text{skin}} D_o\{r_h\} + 0.5\ \pi r_h D_p\{1\}} \right] \tag{A.4}$$

In all these equations, the effective diffusion coefficient D_p is not defined further. It is a function of the ratio of the polymer hydrodynamic size to the pore radius. In this article, the following two theories for the description of the effective diffusion coefficient are summarized: the quantitative porous body approach, and the qualitative scaling analysis. Both theories describe D_p as an intricate function of the ratio of polymer hydrodynamic radius to the pore radius. The introduction of these D_p functions into the already complicated integral (A.4) results in a relation that cannot be solved analytically; it is doubtful whether it can be solved numerically: We did not yet find a solution for this ill-posed mathematical problem.

The authors thank R. H. B. Bouma for his help in the derivation.

REFERENCE

A1. Abramowitz, M.; Stegun, I. A. Handbook of Mathematical Functions with Formulas, Graphs, and Mathematical Tables, 10th printing; Wiley: New York, 1972; p. 11, nr. 3.3.7.